Global NEST Journal, Vol 26, No 3, 05135

Permeability characteristics and mechanism of tungsten tailings treated by the acid solutions

Shanmei Li[a]*, Bingxiang Lin B.S.[b], Weiyi Huang B.S.[c], Kaiqin Wei B.S.[d], Qixiang Wang B.S.[e] and Youlin Zhang B.S.[f]
[a]Department of Civil Engineering and Architecture, Guilin University of Technology, Guilin 541004, China.
[b]China Railway 19 Bureau Group Guangzhou Engineering Co., LTD, Guangzhou 511458, China.
[c]China Communications Construction second highway Engineering Bureau seven engineering Co., Ltd, Nanning 530220, China.
[d]China Communications Construction second highway Engineering Bureau first engineering Co., Ltd, Wuhan 4300000, China.
[e]China Construction Fifth Bureau, Changsha 410019, China.
[f]China Railway First Group construction and Installation Engineering Co., Ltd, Shaanxi 710000, China.
Received: 10/05/2023, Accepted: 08/02/2024, Available online: 26/02/2024
*to whom all correspondence should be addressed: e-mail: lishanmei@glut.edu.cn
https://doi.org/10.30955/gnj.005135

Graphical abstract

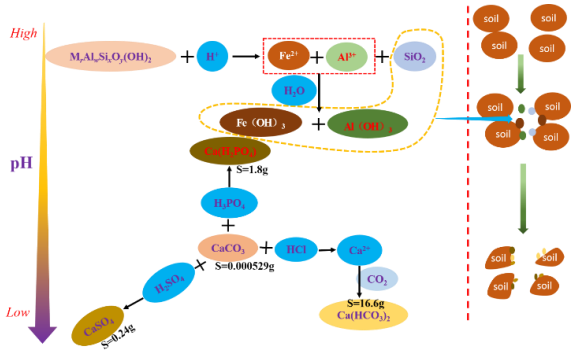

Abstract

Most of the tungsten tailings (TTs) are filled in the open. As a result, the phenomenon that acid rain influences the engineering geological characteristics of tungsten tailings is impossible to avoid, especially in southern China, where acid rain occurs frequently. This work studied the permeability properties of TTs treated with different acid solutions. The HCl, H_2SO_4, and H_3PO_4 solutions were prepared as the permeate fluids with pH values of 7, 5, 4, and 3. The falling head permeability test studied the TTs' permeability characteristics under different acid solutions action. The microscopic mechanism of the movement of the acid solutions and TTs was analyzed based on X-ray diffraction results and nuclear magnetic resonance. The experimental results show that the permeability coefficient of TTs decreases first and then increases with the pH value of HCl and H_2SO_4 solutions and first increases and then decreases and then increases with the pH value of H_3PO_4 solutions. When the pH value >3, the effect of acid on the permeability coefficient is satisfied with HCl >H_2SO_4> H_3PO_4; otherwise, it is satisfied with H_2SO_4> H_3PO_4> HCl. The development law of T_2 spectrum distribution is consistent with the permeability coefficient of TTs treated with the same acid solution. The acid solutions react with chlorite and calcite in the tailings, which affects the permeability of TTs treated by the acid solution. Therefore, preventing the infiltration of acid solutions from entering the tailings is conducive to improving the stability of tungsten tailings dams.

Keywords: Permeability coefficient, acid solution, tungsten tailings.

1. Introduction

Acid rain is a global environmental pollution problem and arouses the attention of many countries worldwide (Seip 2004; Smith 1872; Frediric 2004; Thorjric 1999). Many research results show that acid rain alters the structure, and the physical and mechanical properties of the soil (Ivan 2013; Zeinab 2016). Some workers studied the volume change behavior of soils (Al-Omari R.R., Mohammed W.K., Nashaat I.H., Kaseer O.M. 2007). The effect of sulphuric and phosphoric acids on the behavior of a limestone foundation is remarkable (Parfitt 2011; Prasad 2017). All relevant research results show that acid rain or acid solution significantly affects geotechnical engineering properties (Jiang 2023; Sari 2023; Ji 2023). Tailings are a geotechnical material that stack in the open air. The stability of the tailings dam will be affected by the change of tailings engineering properties under the action of acid rain. So many researchers focus on the impact of acid rain on the engineering properties of tailings.

New pores are created in the tailings as acid rain dissolves some minerals from the mine waste residue (Yang 2009). In addition, acid rain promotes the destruction of the solidified body structure through wetting and drying cycles (Wei 2019). Both of the above reasons change in tailings permeability. In general, the permeability coefficient of tailings gradually increases with the decrease of the solution pH value (Yang 2021). For example, when the sample was soaked in HCl solution for less than 24 hours, the permeability of the model increased significantly; when

soaking for more than 24 hours, the permeability decreased first, then stabilized (Zhang 2017). However, the permeability coefficient soaking in distilled water is almost constant (Zhang 2017). In addition, the effect of acid on soil permeability is inversely correlated with its dry density (Yang 2021). The existing studies showed that the affection of the tailings permeability treated with the acid solution was significant.

The main environmental problems caused by the dam mainly include:

- Environmental pollution is led by heavy metal precipitation (Wang 2014).
- Mudslides are caused by the migration of tinny particle content (Shi 2020).
- Dam instability.

The above problems are related to the permeability of the soil. By their very nature, the core of the tailings' dam disaster is the change of seepage, stress, and chemical field. Therefore, studying the permeability characteristics of tailings reservoirs is one of the compelling methods of revealing the mechanism of tailings dam failure. It also can provide a theoretical basis for migrating and preventing pollutants.

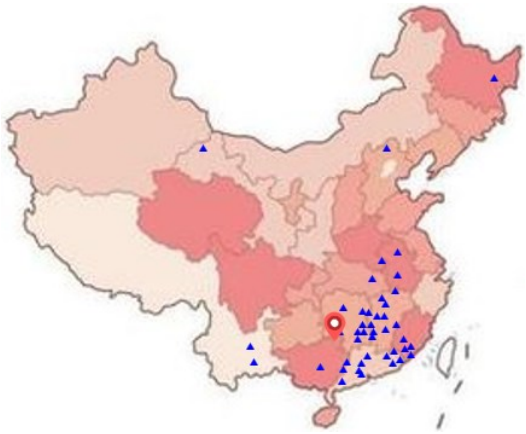

Figure 1. Map of tungsten ore distribution in China

The tungsten ore resources are rich in China's central and southern regions (see Figure 1). It means a large amount of tailings waste. Open-pit backfilling, as a simple method, is the primary way to dispose of tailings. The mountains are very steep in the south of China, and many people still live in rural areas in the mountains. Once the fillings are unstable, it will cause irreparable loss to life, property and environment. The soil filling and the climate change the stress, seepage, and chemical fields in the open-pit backfilled tailings reservoir. Southern China is an area where acid rain is widespread. However, work considering the effect of the acid solution on permeability characteristics and the action mechanism of TTs has yet to be studied meticulously. To fill this gap, a series variable head permeability tests were done to check the permeability characteristics of TTs under the action of hydrochloric acid, sulfuric acid, and phosphoric acid with different pH values. To explain the test results and obtain the influence mechanism, several microstructural (e.g., NMR measurements and XRD profiles) were also undertaken on TTs treated with the different acid solutions. Finally, this work aims to provide theoretical guidance for the stability of tailings reservoirs.

2. Experimental materials and methods

2.1. Materials characterization

The primary materials are TTs, sulfuric acid, hydrochloric acid, and phosphoric acid. The TTs were from Guilin, South China, a gray powder with a specific gravity of 2.76. Figure 2 shows the grading curve. The particles are fine and uniform. More than 71% of the particles were distributed between 0.075mm and 0.25mm. Therefore, it is a mealy sand according to the grain composition. The original soil sample is very loose and crumbled quickly, with an initial moisture content of about 13%. X-Ray diffraction (XRD) tested the mineral compositions of TTs (see Table 1). Quartz, calcite, essonite, and pyroxene are the main in TTs. At the same time, the fluorescence spectroscopy tested the principal metallic oxides of TTs (see Table 2). Table 2 shows that SiO_2, CaO, Fe_2O_3, and Al_2O_3 are the main in TTs, more than 88%.

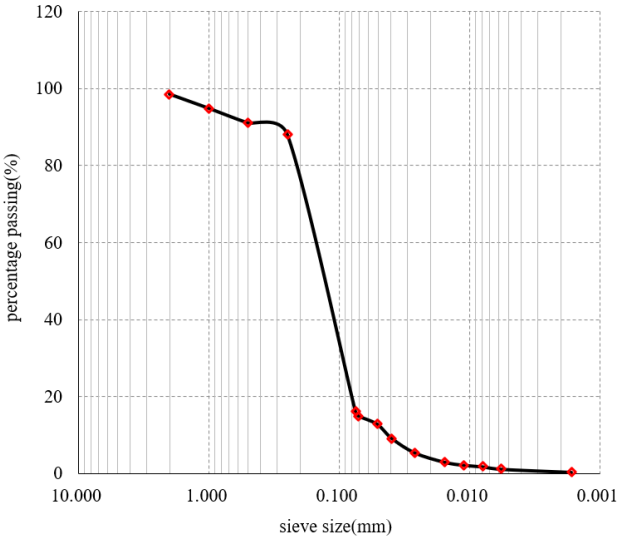

Figure 2. Particle grading curve of tungsten tailings

Table 1. Main mineral composition of tungsten tailings

Mineral composition	Content/%	Mineral composition	Content/%
quartz	43	grossular	7
plagioclase	2	pyroxene	6
microcline	3	amphibole	1
calcite	31	Total clay	5
fluorite	1		

Table 2. Main metal oxide types of tungsten tailings

Oxide composition	Content/%	Oxide composition	Content/%
SiO_2	40.05	MnO	0.68
CaO	29.30	TiO_2	0.41
Fe_2O_3	12.42	WO_3	0.30
Al_2O_3	6.90	BaO	0.29
MgO	4.33	PbO	0.24
K_2O	2.12	SnO_2	0.16
SO_3	1.67	Cs_2O	0.08
P_2O_5	0.70		

2.2. Sample preparation and experimental procedure

As shown in Figure 3, the method of this study is illustrated by the work-flow chart. Firstly, the ring knife samples were prepared and saturated in the distilled water. Then the osmotic coefficient of the samples in the distilled water and the different acid solution were tested by the variable head permeability test. Lastly, the microscopic properties of the specimens treated with different acidic solutions were tested by the nuclear magnetic resonance (NMR) and the X-ray diffraction (XRD) respectively.

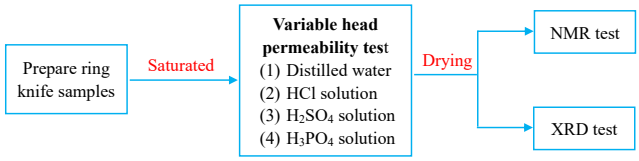

Figure 3. Work-flow chart

The TTs were crushed and screened through 10 mesh after drying in an oven at 105°C for 24 hours according to the Standard for soil test method (GB/T 50123-1999). We weighed 192 g TTs, then pressed them into the ring cutter to prepare the sample with a height of 4 cm and a diameter of 6.18 cm by a computerized electronic universal testing machine. The dry density of the pieces was kept around 1.6 g/cm^3. Then the soil samples with the cutting ring were fixed in the laminated saturator and put into the vacuum tanker. Lastly, the soil sample is vacuumed and saturated in distilled water.

As you know, it is easy to control the void ratio of a soil sample but impossible to control the pore structure. The void ratio and the pore structure decide the soil's permeability. The permeability coefficients of the soil sample under the same acid solution with different pH values (e.g., 3, 4, 5, 7) were tested by the same soil example to avoid the test error caused by the sample preparation. The test process under different acids is consistent, so only the osmotic test process under hydrochloric acid solution is introduced in detail here. (I) Firstly, tested the permeability of the sample under the act of distilled water (pH 7); (II) Next, changed the permeability solution with the hydrochloric acid solution of pH 5 and kept it seeping out from the top of the sample until the pH value of the exudate solution remained constant; then tested the permeability coefficient under the action of pH 5; (III) Lastly, change the acid solution with pH 4 and pH 3 successively, and repeat the process (II) to test the permeability coefficient of the sample treated with the pH 4 and the pH 3 solution, respectively. The other permeability coefficient of the sample under the action of the sulfuric and the phosphoric acid solutions was tested in the same way as these details. Two parallel tests were considered for each group to ensure test accuracy. The operation processes of the falling head permeameter test were completed according to the Standard for soil test method (GB/T 50123-1999). The nuclear magnetic resonance and the XRD diffraction method test the microstructure after the permeability test.

3. Experimental results and discussion

3.1. Osmotic characteristics

Figure 4 shows the TTs' permeability coefficient under different acid solutions' actions. The initial permeability coefficients of samples were quite different though the initial void ratio is the same. The permeability coefficients decreased slightly first and then increased with the decrease of HCl and H_2SO_4 solution pH value, and first increased somewhat, then reduced and then advanced with the H_3PO_4 solution pH value. Since the initial permeability coefficient of the samples are quite different, it is difficult to compare the influence of different acid types on the permeability coefficient of TTs only by the permeability coefficient. In order to solve this problem and eliminate the chemical effects of the acid solution on the TTs, the concept of gradient of permeability coefficient was introduced. It is expressed by the Formula 1.

$$\Delta ki = \frac{k_i - k_7 1}{k_7} \times 100\%, (i = 7,5,4,3) \quad (1)$$

Where Δk_i is the gradient of permeability coefficient, k_i is the permeability coefficient of the sample effected by the acid solution with pH i, k_7 is the permeability coefficient when the solution is distill water.

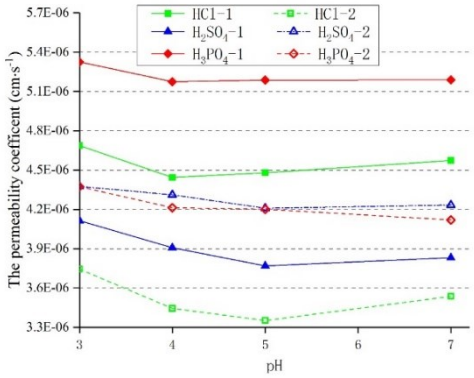

Figure 4. Permeability coefficient at different pH values

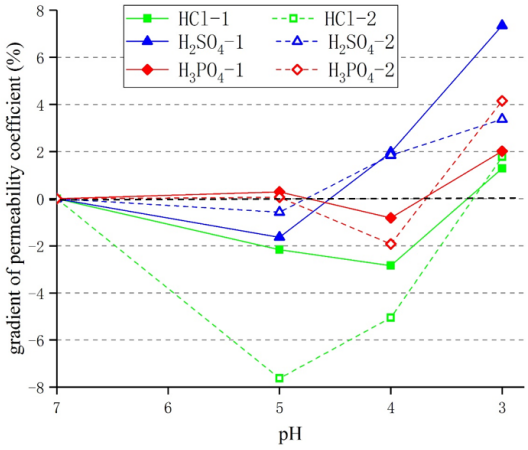

Figure 5. Gradient of permeability coefficient at different pH values

Figure 5 shows the gradient of the permeability coefficient calculated by Equal 1. As shown in Figure 5, the effect of different acids on the permeability coefficient changed with the pH value. Properly speaking, the impact of various

acids solution on the permeability coefficient of TTs do with HCl>H_2SO_4>H_3PO_4 when the pH value decreases from 7 to 4 and with H_2SO_4>H_3PO_4>HCl when the pH value drops to 3. Meanwhile, the smaller the initial permeability coefficient (pH=7), the more significant the change of the permeability coefficient in the acid solutions by comparing with Figures 4 and 5.

3.2. Characteristics of the T_2 relaxation curve

Nuclear magnetic resonance (NMR) is a technique for nondestructive analysis of the internal structure of materials. The principle of its operation is that the magnetic field of the nucleus spin itself is rearranged under the applied magnetic field, and the spin of the nucleus will be in a low-energy state. By emitting radiofrequency pulses at a particular frequency to the tungsten tailings in the magnetic field, the hydrogen atom nucleus will undergo magnetic resonance to reach the non-equilibrium state of high energy state. After the RF pulse stops, the hydrogen nucleus changes from high-energy state to a low-energy state to release energy in relaxation. A specific technique detects the NMR signal in relaxation to obtain the transverse relaxation time T_2 spectrum. T_2 can be expressed by Formula 2 (Yu 2013).

$$\frac{1}{T_2} = \rho_2 \frac{S}{v} = \rho_2 \frac{\alpha}{R} \quad (2)$$

Where ρ_2 is the transverse relaxation rate, μm/s, which is related to the physicochemical properties of the soil particles surface; s is the pore surface area, μm^2; v is the pore water volume, μm^3; R is the pore radius of the soil.

The transverse relaxation time T_2 is closely related to the pore size, shape, surface characteristics, etc. The position of the peak T_2 on the relaxation timeline is proportional to the pore radius, and the ordinate coordinate is related to the number of the pore's volume. The peak of T_2 is proportional to the pores volume corresponding to pore size if the fluid properties are the same.

Fig.6 shows the relaxation spectrum of TTs samples. As seen in Figure 6, the most curve of the specimens appeared bimodal, with one prominent peak and one secondary peak, except for the piece of H_2SO_4-2. The sample curve of H_2SO_4-2 exhibited three mountains, with one central peak and two small secondary peaks. The prominent peak of all curves is mainly distributed in 0.1 ms~4 ms, and the secondary peak is mainly distributed in 50 ms~1250 ms. The area of the principal peak is much larger than that of the secondary peak. This means that most pores are tiny in TTs. The permeability of TTs considering the chemical reaction by acid solution was focused on according to the characteristics of the T_2 relaxation curve in this paper. It cannot be ignored that the H ion in the acid solution affects the NMR diffraction. However, the ionization constants of hydrochloric acid, sulfuric acid, and phosphoric acid are different. In other words, the numbers of hydrogens in the acid solutions with HCl, H_2SO_4, and H_3PO_4 are different, even though the pH value is the same. Therefore, T_2 of the samples treated with the same acid solution was compared and analyzed. As seen in Figure 6, the T_2 curve areas of samples treated with the same acid solution followed the rules with HCl-1> HCl-2, H_2SO_4-2>H_2SO_4-1, and H_3PO_4-1>H_3PO_4-2. By comparing Figure 4, the variation rule of the T_2 curve area is consistent with the permeability coefficient.

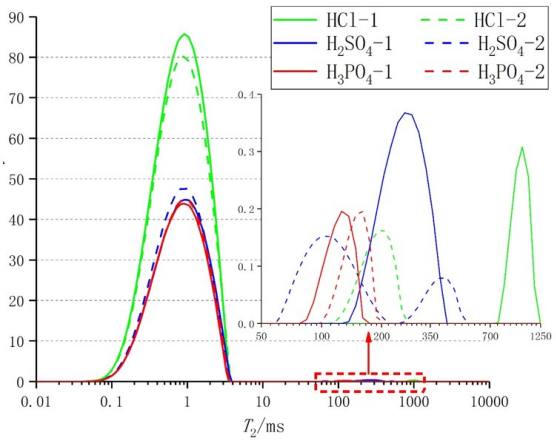

Figure 6. T_2 relaxation curve of tungsten tailings treated by the three acid solutions

3.3. XRD diffraction

Figure 7 shows the XRD diffraction pattern of tungsten tailings treated by the acid solutions. The main mineral components of the TTs are quartz, calcite, clinochlore, muscovite, and grossularite. Obviously, the position of all diffraction peaks has no change but a few peaks (e.g. calcite and clinochlore) are significantly weakened when the samples are treated with the HCl and H_2SO_4 solutions. It can be seen that the chemical sensitivity of chlorite to hydrochloric acid is more potent than that of sulfuric acid, but that of calcium is the opposite by comparing the peak strength of clinochlore and calcite. The peak intension corresponding to 29.5° (2θ) is significantly enhanced (see the blue line). The peak corresponds to the calcite and the calcium hydrogen phosphate. The increase of this peak intensity is the generation of the latter because the H_3PO_4 solution reacts with calcite from the TTs to form $Ca(H_2PO_4)_2$.

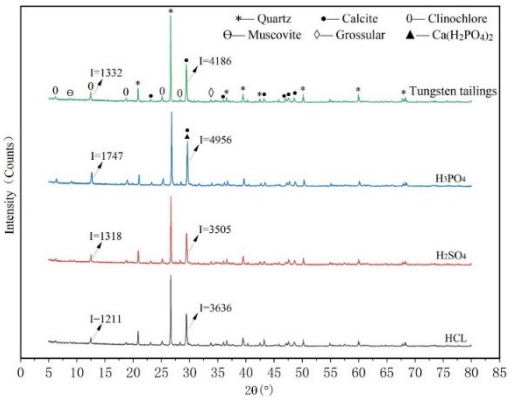

Figure 7. XRD diffraction curve

4. Discussion

The results of permeability test show that the permeability coefficients decreased slightly first and then increased with the decrease of HCl and H_2SO_4 solution pH value, and first increased somewhat, then reduced and then advanced with the H_3PO_4 solution pH value. It is obviously that it is

different with the studies in the literature (Yang 2021; Zhang 2017) mentioned above. In addition, the laws of permeability coefficient of tungsten tailings treated with H_2SO_4 or H_3PO_4 solution are not clear. It is necessary to deeply discuss the influence of different acid solutions on the permeability coefficient of tungsten tailings.

4.1. The action mechanism of HCl solution

According to the results of XRD, clinochlore, a robust hydrochloric acid sensitivity, is one of the mineral compositions of TTs (Xu 2016). Clinochlore's composition is complex. Its molecular formula can be expressed as $M_rAl_wSi_xO_y(OH)_2$, where the subscript is the atomic number, M is for Mg and Fe atoms, and Figure 8 shows the molecular structure.

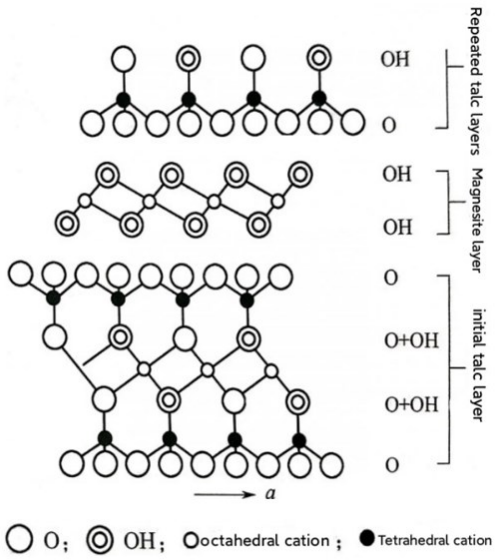

Figure 8. Molecular structure of clinochlore

The structure of clinochlore contains the interlayer and the 2:1 octahedral sheets, which is trioctahedral. The clinochlore structure comprises regularly stacked, negatively charged 2:1 layers with a single layer of positively charged interlayer octahedral connected by H-bonds. The tetrahedral cations are mainly Si^{4+}, and the octahedral cations are mainly Mg^{2+} and Fe^{2+}. The interlayer octahedral sheet comprises either a trioctahedral (Mg) or dioctahedral arrangement of oxyhydroxides. The strength of the Si-O bond is greater than that of M-O (M is a metal element) because Si is a tetravalent ion, but the most charged metal ions are trivalent. Therefore, M-O is easily broken in the acid solution to release Mg^{2+} and Fe^{2+}. Clinochlore reacts with H ion as follows,

$$M_rAl_wSi_xO_y(OH)_2+H^+ \rightarrow rM^{2+} + wAl^{3+} + xSiO_2\cdot 2H_2O+ H_2O \quad (3)$$

The amorphous SiO_2 colloid generates according to Formula 3. A low concentration of SiO_2 colloid prompt to carry fine particles in minerals to migrate with water flowing. It is easy to block the permeability channel and reduce the permeability coefficient. In addition, the dissolved Fe^{2+} is oxidized with the pH of the solution increases for the H ion is consumed, and the following reactions occur

$$4Fe^{2+} + O_2+10H_2O \rightarrow 4Fe(OH)_3\downarrow +8H^+ \quad (4)$$

The $Fe(OH)_3$ are insoluble in weak acids, thereby blocking the pores and reducing the infiltration capacity. According to the above analysis, the H ion first reacts with clinochlore to generate amorphous SiO_2 and $Fe(OH)_3$. Both lead to a decrease in the permeability coefficient of tungsten tailings, when the pH value of the hydrochloric acid solution is higher. However, $Fe(OH)_3$ is dissolved as the concentration of the acid solution increases (see Formula 5).

$$Fe(OH)_3\downarrow +3HCl=FeCl_3+3H_2O \quad (5)$$

At the same time, the excess acid solution reacts with calcite, as in the Formula 6.

$$CaCO_3+2HCl=CaCl_2+CO_2\uparrow +H_2O \quad (6)$$

Due to the dissolution of $Fe(OH)_3$ and $CaCO_3$, the porosity of TTs increases, and the permeability coefficient increases. The reaction law of hydrochloric acid with chlorite and calcite is consistent with the results of the infiltration and XRD experiments.

4.2. The mechanism of action of H_2SO_4 solution

According to the XRD diffraction pattern, the clinochlore content of TTs treated with an H_2SO_4 solution decreased. It proves that clinochlore is also sensitive to H_2SO_4, which is the main reason for the decrease in the permeability coefficient of TTs treated with the weak H_2SO_4 solution. Its reaction mechanism is the same as HCl. In addition, the H_2SO_4 solution can react with calcite (see Formula 7)

$$CaCO_3+H_2SO_4==CaSO_4+CO_2\uparrow +H_2O \quad (7)$$

The solubility of $CaSO_4$ is 0.24g/100 g water, which is a slightly soluble substance. The generated $CaSO_4$ covers the surface of calcite to prevent the reaction of Formula 7. It can be ensured that the molar mass of $CaCO_3$ consumed by the response is the same as the $CaSO_4$ generated. Whereas the group of $CaSO_4$ developed is more than that of $CaCO_3$ consumed because the molecular weight of the former is more significant. Furthermore, considering that the density of these two substances is about 2.96g/cm^3, the volume of $CaSO_4$ generated is more effective than that of $CaCO_3$ consumed, which leads to reduce the pores and permeability capacity of TTs. As the pH value of the solution decreases, more calcite reacts with sulfuric acid, and a large amount of CO_2 and heat is produced with the reaction. CO_2 is challenging to escape from the sample because it is wrapped in a thin film. Therefore, CO_2 reacts with $CaCO_3$, as shown in Formula 8.

$$CaCO_3+CO_2+H_2O==Ca(HCO_3)_2 \quad (8)$$

The solubility of $Ca(HCO_3)_2$ is 16.6 g/100 g water, much more excellent than of $CaCO_3$ which is 0.00052g/100 g water. It is remarkable that the reaction of Formula 8 is in favor of improving the permeability capacity of TTs.

4.3. The mechanism of action of H_3PO_4 solution

Phosphoric acid is a triprotic acid with $K_{a1}=7.5\times10^{-3}$, $K_{a2}=6.2\times10^{-8}$, and $K_{a3}=4.8\times10^{-13}$. Carbonic acid is a diacid acid with $K_{a1}=4.3\times10^{-7}$, $K_{a2}=5.6\times10^{-11}$. So phosphoric acid can only react with $CaCO_3$ according to formula 9.

$$2H_3PO_4+CaCO_3\rightarrow Ca(H_2PO_4)_2+CO_2\uparrow+H_2O \quad (9)$$

XRD has confirmed $Ca(H_2PO_4)_2$ in TTs treated with the H_3PO_4 solution (see the blue line in Figure 5). The solubility of $Ca(H_2PO_4)_2$, which is 1.8g/100 g water, is greater than that of $CaCO_3$. It's undoubtedly that the reaction of $CaCO_3$ increases the porosity of tungsten tailings to improve the permeability coefficient. Chemical reactions (formula 9) are more likely to proceed in lower pH value environment. However, the excess $Ca(H_2PO_4)_2$ precipitates if it continues to produce with the decrease of the pH value. It leads to blocking the channel and decreases the permeability coefficient. When the pH value is low enough (e.g., pH 3), a large amount of CO_2 and heat are produced by chemical reactions (Formula 9). Meanwhile, the CO_2 generated promotes the production of $Ca(HCO_3)_2$ (Formula 8). Due to the higher solubility of $Ca(HCO_3)_2$, the pores and the permeability are improved.

5. Conclusions

The falling head permeability test studied the permeability properties of TTs treated with different acid solutions. The HCl, H_2SO_4, and H_3PO_4 solutions as the permeate fluids with pH values of 7, 5, 4, and 3 were prepared. X-ray diffraction and nuclear magnetic resonance analyzed the microscopic mechanism of the interaction between acid solution and TTs. The following conclusions are obtained with the infiltration and microscopic characteristics.

1. The permeability coefficient of TTs decreased first and then increased with the pH value of the hydrochloric acid and the sulfuric acid solution, and first increased, then fell and rose again with the decline of the pH value of the phosphoric acid solution.

2. The effect of acids on the permeability coefficient follow $HCl>H_2SO_4>H_3PO_4$ when the $pH\geq4$, and follow $H_2SO_4>H_3PO_4>HCl$ when pH=3.

3. The denser the tungsten tailings, the greater the effect of the acidic solution on its permeability.

4. For the same acid, the variation rule of T_2 in the NMR curve is consistent with the variation rule of the permeability coefficient.

5. Higher pH value of HCl and H_2SO_4 solution reduce the permeability coefficient by dissolving chlorite to produce amorphous SiO_2 and $Fe(OH)_3$, while lower pH value of HCl and H_2SO_4 dissolve calcite to increase the permeability coefficient; H_3PO_4 solution mainly reacts with calcite and affects the permeability of tungsten tailings.

The current study only focuses on the permeability of saturated samples in different acid solutions. As a result, the permeability characteristics changed obviously in other acid solutions. However, it should be undoubled that the TTs filled in the field are affected by dry-wet cycles. This cycle changes the crack distribution in the tailings. Some works are still in progress to consider the permeability of TTs in different acid solutions by dry-wet processes.

Acknowledgements

The authors wish to acknowledge the financial support from the National Natural Science Foundation of China (NSFC) under Grants No. 52268055, the Natural Science Foundation in Guangxi under Grant No. 2022JJB160082, Guangxi Program of Key Laboratory of Geo-mechanics and Engineering Grant No.19-Y-21-3.

Conflict of interest statement

The data that support the findings of this study are available from Shanmei Li upon reasonable request. The work is done by the authors. There is no conflict of interest with any other people or organization.

References

Frediric C.M, Hans M.S. (2004). Acid rain in Europe and the United States: an update. Environmental Science & Policy, **7**, 253–265.

Haiqiang J, Jing H, Lei R, Zenbang G, Erol Y. (2023). Study of early-age performance of cementitious backfills with alkali activated slag under internal sulfate attack. Construction and Building Materials, **371**, 130786.

Ivan G, Ikuo T. (2013). Stress-strain characteristics of two natural soils subjected to long-term acidic contamination. Soils and foundations, **53(3)**, 469–476.

Menz, F.C. Seip, H.M. (2004). Acid rain in Europe and the United States:an update. Environmental Science & Policy, **(7)**, 253–265.

Muhammet S, Erol Y, Tugrul K. (2023). Long-term ageing characteristics of cemented mine backfill: Usability of quarry sand as a partial substitute of hazardous tailings. Journal of Cleaner Production, In-Press. https://doi.org/10.1016/j.jclepro.2023.136723.

Parfitt M.K, Jones D.J, Garvin R.G. (2011). Structural, construction, and procedural failures associated with long-term pyritic soil expansion at a private elementary school in Pennsylvania. J. Perform. Constr. Facil, **25(1)**, 56–66.

Prasad C.R, Reddy P.H, Murthy V.R, Sivapullaiahb P.V. (2017). Swelling characteristics of soils subjected to acid contamination. Soils and Foundations, **58**, 110–121.

Shi Y.Q, Li C.H, Long D.Y. Study on mesoscopic structural characteristics of osmotic failure of fine-grained tailings sand [J]. Journal of Xi'an Jiaotong University, 2020, **54(04)**, 155–164.

Thorjric C.M, Hans M.S, Arne S, Jan M, Ivar P.M, Rolf D.V, Espen L, Valter A, Tang D.G, Odd E. (1999). Acid deposition and its effects in China: an overview. Environmental Science & Policy, **(2)**, 9–24.

Wang J, Liu Y, Zhang Z.J, Gui R. (2014). Effect of rainfall infiltration on the stability of tailings dams. Journal of University of South China (Natural Science Edition), **28(01)**, 24–28, DOI: 10.19431/j.cnki.1673-0062.2014.01.007.

Wei M.L, Zhang Z, Li Y.Y, Jia S.B. (2019). Effect of acid rain on dry and wetness of cured fine iron tailings sand of alkali excitation materials. Non-Metallic Ore, **42(05)**, 76–78.

Xu M.B, Liu W.H, Wen S.C. (2016). Modern reservoir protection technology. Wuhan: China University of Geosciences Press.

Xubo J, Xiaozhong G, Zhuoran W, Shuai X, Hai J, Eeol Y. (2023). Admixture effects on the rheological/mechanical behavior

and micro-structure evolution of alkali-activated slag backfills. Minerals, **13(1)**, 30.

Yang B.Y, Chen Z.C, Wu F.H. (2009). Simulation study on environmental pollution and treatment of tailings. Environmental Science and Technology, **32(9)**, 164–166. DOI: 10.3969/j.issn.1003-6504.2009.09.038.

Yang J., He Y, Li B.B, Hu G. (2021). Study on osmosis characteristics and pollution prevention and control of a tailings sand under the action of chemical factors. Metal Mine, **(09)**, 184–191. DOI: 10.19614/j.cnki.jsks.202109026.

Yu S.Y, Shao L.T, Liu S.Y. (2013). Stability analysis of tailings dam body based on finite element limit equilibrium method. Geotechnical Mechanics, **34(4)**, 1185–1190.

Zeinab B, Afshin A, Bujang B.K.H, Sridharan A, Satoru K. (2016). Effect of acid rain on geotechnical properties of residual soils. Soils and foundations, **56(6)**, 1008–1020.

Zhang Y, Zhang B, Bing L, Zhang E.J. (2017). Effect of acid-base solution on permeability characteristics of sulfur-containing tailings sand. Nonmetallic Ore, **40(06)**, 48–50.